

# Vapor-film-unit model and heat transfer correlation for natural-convection film boiling with wave motion under subcooled conditions

SHIGEFUMI NISHIO and HIROYASU OHTAKE

Institute of Industrial Science, University of Tokyo 7-22-1, Roppongi, Minato-ku, Tokyo 106, Japan

(Received 24 August 1992 and in final form 27 November 1992)

**Abstract**—This report presents a heat transfer model and correlation of natural-convection film-boiling heat transfer with interfacial wave motion under subcooled conditions. First, the vapor-film-unit model developed for saturated film boiling in our previous report was extended to subcooled film boiling along inclined and vertical flat-plates and also around horizontal cylinders of large diameter. Next, based on the vapor-film-unit model, a general form of heat transfer correlation of film boiling with wave motion was developed. Comparison with experimental data showed that the present heat transfer model and correlation can predict the effects of the fluid properties, liquid subcooling, wall superheat, the geometry and the size of the heat transfer surface on film-boiling heat transfer with wave motion.

## 1. INTRODUCTION

NATURAL-CONVECTION film-boiling heat transfer is encountered in a variety of engineering fields such as cooling of superconducting magnets, cooldown of cryogenic systems, core safety of light water reactors, heat treatment of steel and glass, and rapid solidification processing, and a number of analytical, numerical and experimental studies have been reported as reviewed by Kalinin *et al.* [1].

It is well known that natural-convection film-boiling heat transfer depends on the geometry and the size of the heat transfer surface. For example, Breen and Westwater [2] investigated saturated film-boiling around horizontal cylinders of various diameters, and they found that the saturated film-boiling heat transfer can be classified into small-, middle-, and large-diameter regions. The middle-diameter region is the cylinder-diameter region in which experimental data of the averaged heat-transfer coefficient of saturated film boiling are in good agreement with the prediction by Bromley's analysis [3]. In the small-diameter region, experimental data are higher than the prediction by his analysis. The large-diameter region is the diameter region in which experimental data are higher than the prediction and they are independent of the diameter.

Bromley's analysis was extended to the so-called two-phase boundary-layer (TPBL) theory by Nishikawa *et al.* [4–6] by taking into account the effects of liquid subcooling and temperature dependence of the fluid properties. The TPBL theory assumes basically the film boiling situation in which the vapor film is laminar and smooth. Sakurai *et al.* [7] conducted film boiling experiments with horizontal cylinders over a

wide range of liquid subcooling and system pressure, and they confirmed that the TPBL theory correctly predicts the respective effects of liquid subcooling, system pressure, and the cylinder diameter on the film-boiling heat transfer in the middle-diameter region. It was also found by Frederking and Clark [8], Dhir and Purohit [9], and Farahat and Nasr [10] that the TPBL theory is applicable to film boiling around spheres of middle diameter. Nishio *et al.* [11] conducted film boiling experiments with horizontal flat-plates facing downward, and they showed that the vapor film was classified into a glassy smooth film and a wavy film and a heat transfer analysis assuming the laminar-smooth vapor film was applicable to saturated film boiling from horizontal flat-plates facing downward as long as the vapor film remained smooth. It can be thus concluded that all the film boiling systems mentioned above belong to film boiling with the laminar-smooth vapor film. The feature of film boiling of this type is that the heat transfer coefficient relates basically to the surface size. Film boiling of this type is expected to appear also in film boiling along short vertical plates.

For saturated film boiling around horizontal cylinders in the large-diameter region, Breen and Westwater [2] observed the development of wave motion on the vapor-liquid interface around the perimeter. Such interfacial wave motion was reported also for saturated film boiling on horizontal flat-plates facing upward by Hosler and Westwater [12] and along high vertical-surfaces by Hsu and Westwater [13], Suryanarayana and Merte [14], Greitzer and Abernathy [15], Bui and Dhir [16] and Nishio *et al.* [17]. Most of these studies show that the time-averaged local heat-transfer coefficient of saturated film boiling

## NOMENCLATURE

$a_v$	constant relating to vapor velocity	<b>Greek symbols</b>	
$a_l$	constant relating to liquid velocity	$\beta$	volumetric expansion coefficient [ $\text{K}^{-1}$ ]
$B$	buoyancy parameter, $c_{p\text{lf}}/\beta L$	$\delta_v$	vapor film thickness [m]
$c_p$	specific heat [ $\text{kJ kg}^{-1} \text{K}^{-1}$ ]	$\delta_l$	thickness of boundary layer in liquid [m]
$D$	diameter of cylinder [m]	$\delta$	$\delta_v/\delta_l$
$F$	constant relating to liquid velocity	$\eta$	location of vapor–liquid interface under disturbance [m]
$g$	gravitational acceleration [ $\text{m s}^{-2}$ ]	$\eta_0$	amplitude of disturbance on vapor–liquid interface [m]
$Gr_v$ [s]	Grashof number of vapor flow, $g\rho_{\text{vf}}(\rho_{\text{lf}} - \rho_{\text{vf}})s^3/\mu_{\text{vf}}^2$	$\lambda$	vapor–film–unit length [m]
$Gr_l$ [s]	Grashof number of liquid flow, $g\rho_{\text{lf}}(\rho_{\text{lb}} - \rho_{\text{lf}})s^3/\mu_{\text{lf}}^2$	$\lambda_{\text{c,RT}}$	critical wavelength of Rayleigh–Taylor instability, $2\pi\lambda_0$ [m]
$h$	local heat-transfer coefficient [ $\text{W m}^{-2} \text{K}^{-1}$ ]	$\lambda_{\text{d,KH}}$	most dangerous wavelength of Kelvin–Helmholtz instability [m]
$h_{\text{av}}$	heat transfer coefficient averaged over surface [ $\text{W m}^{-2} \text{K}^{-1}$ ]	$\lambda_{\text{d,RT}}$	most dangerous wavelength of Rayleigh–Taylor instability, $2\pi\sqrt{(3)}\lambda_0$ [m]
$h_{\text{sat}}$	averaged heat-transfer coefficient to saturated liquid [ $\text{W m}^{-2} \text{K}^{-1}$ ]	$\lambda_0$	Laplace capillary length, $\sqrt{(\sigma/g(\rho_{\text{ls}} - \rho_{\text{vs}}))}$ [m]
$h_{\text{sub}}$	averaged heat-transfer coefficient to subcooled liquid [ $\text{W m}^{-2} \text{K}^{-1}$ ]	$\mu$	viscosity [Pa s]
$k$	thermal conductivity [ $\text{W m}^{-1} \text{K}^{-1}$ ]	$\bar{\mu}$	$\mu_{\text{vs}}/\mu_{\text{ls}}$
$L$	latent heat of vaporization [ $\text{kJ kg}^{-1}$ ]	$\nu$	kinematic viscosity [ $\text{m}^2 \text{s}^{-1}$ ]
$L^*$	modified latent heat of vaporization, $L + 0.5c_{p\text{vf}}\Delta T_{\text{sat}}$ [ $\text{kJ kg}^{-1}$ ]	$\rho$	density [ $\text{kg m}^{-3}$ ]
$m$	wave-number [ $\text{m}^{-1}$ ]	$\bar{\rho}$	$\rho_{\text{vs}}/\rho_{\text{ls}}$
$m_d$	wave-number of most dangerous wavelength [ $\text{m}^{-1}$ ]	$\sigma$	surface tension [ $\text{N m}^{-1}$ ]
$Nu$ [s]	Nusselt number, $h_{\text{av}}s/k$	$\Phi$	fluctuation of velocity potential
$Pr$	Prandtl number	$\phi$	inclination angle relative to horizontal downward plane
$Sb$	subcooling parameter, $c_{p\text{lf}}\Delta T_{\text{sub}}/L$	$\phi_n$	angular location of $n$ th vapor dome
$Sp$	superheat parameter, $c_{p\text{vf}}\Delta T_{\text{sat}}/L$	$\phi_{\text{st}}$	maximum angle of stable vapor film
$Sp^*$	modified superheat parameter, $Sp/(1 + 0.5Sp)$	$\omega$	angular frequency [ $\text{s}^{-1}$ ].
$s$	representative length [m]	<b>Subscripts</b>	
$\Delta T_{\text{sat}}$	wall superheat [K]	ex	experiment
$\Delta T_{\text{sub}}$	liquid subcooling [K]	lb	liquid at bulk temperature
$t$	time [s]	lf	liquid at film temperature
$U$	velocity [ $\text{m s}^{-1}$ ]	ls	saturated liquid
$u_{\text{av}}$	velocity averaged in plane perpendicular to surface	sat	saturated condition
$x$	distance from leading edge [m]	sub	subcooled condition
$y$	distance from vapor–liquid interface [m].	vf	vapor at film temperature
		vs	saturated vapor.

along high vertical-surfaces is independent of the distance from the film-boiling leading edge except for a region near the leading-edge. Since this feature is very different from the prediction by the TPBL theory, two types of models have been proposed to elucidate this feature of saturated film boiling with wave motion. The model of the first type assumes the film boiling situation in which the vapor film is turbulent and wavy. Such a turbulent-wavy model was developed first by Hsu and Westwater [13] and it was extended by Suryanarayana and Merte [14] and Coury and Dukler [18]. On the other hand, the model of the second type assumes the situation in which the vapor film is

wavy but laminar. Such laminar-wavy models were developed for horizontal flat-plates facing upward by Berenson [19] and for high vertical-surfaces by Greitzer and Abernathy [15], Andersen [20] and Bui and Dhir [16]. Following the Berenson's model [19], the Rayleigh–Taylor instability makes the vapor–liquid interface on horizontal flat-plates facing upward to be wavy. This wavy interface divides the vapor film into several cells. Each cell consists of a vapor dome and an adjacent thin-vapor-film. Vapor generated in the thin-vapor-film is absorbed by the adjacent vapor domes without flowing along the whole length of the surface. In this way, the heat transfer process in film-

boiling of this type is almost closed in each cell, and thus the cell is called 'the vapor-film-unit' in this report. In this situation, the length scale governing the heat transfer becomes the vapor-film-unit length, which is determined by the Rayleigh–Taylor instability but not by the surface size. Existence of such vapor-film-units is assumed also in the laminar-wavy models for high vertical-surfaces, but in these models the vapor-film-unit length is related to the Kelvin–Helmholtz instability. In this report, the models based on such vapor-film-units are generally called 'the vapor-film-unit model'. Nishio *et al.* [17] extended the vapor-film-unit model to saturated film boiling along inclined flat-plates and around horizontal cylinders of large diameter, and they claimed that the vapor-film-unit model can predict correctly experimental data of a wide range for the effects of the fluid properties, wall superheat, the surface geometry and the size on saturated film boiling with wave motion. Summarizing these results, it seems reasonable to consider that saturated film boiling with wave motion belongs to film boiling with the laminar-wavy vapor film.

As for saturated film boiling around horizontal cylinders (wires) in the small-diameter region, Nishikawa *et al.* [5] suggested that the boundary-layer approximation employed in the TPBL theory became invalid and this resulted in a deviation from the TPBL theory. On the other hand, Baumeister and Hamill [21] developed a heat transfer model around horizontal thin-wires. They suggested that vapor-film-units lining along the wire caused an axial component in the vapor flow and this resulted in a deviation from the TPBL theory. Nishio and Ohtake [22] conducted film boiling experiments with horizontal thin-wires, and they showed that the saturated film-boiling heat transfer in the small-diameter region were correlated by taking into account both the effects mentioned above. It is thus considered that saturated film boiling around horizontal cylinders of small diameter is also a kind of film boiling with the laminar-wavy vapor film.

Summarizing the above brief review, the laminar-wavy vapor film is expected to appear in saturated film boiling on large horizontal-flat-plates facing upward, long inclined-flat-plates, high vertical-surfaces, and horizontal cylinders of large and small diameter.

On the other hand, since liquid subcooling tends to stabilize the wave motion, it may be possible for liquid subcooling to suppress the enhancement effect caused by the wave motion. It is thus expected that in subcooled film boiling the normal enhancement effect of liquid subcooling competes with such a suppressing effect. For example, Nishio and Ohtake [22] reported experimental results in which the heat transfer coefficient of film boiling around a horizontal thin-wire took a minimum at a certain degree of liquid subcooling for thinner wires. As for the effects of liquid subcooling on film boiling with wave motion, Ohtake and Nishio [23] reported that the wave motion was also observed in subcooled film boiling along high vertical-surfaces and around horizontal cylinders of

large diameter. They also reported experimental data of the time-averaged distribution of the local heat-transfer coefficient of subcooled film boiling in these systems. As far as we know, there is no heat transfer model applicable to subcooled film boiling with wave motion. In this report, the vapor-film-unit model developed previously for saturated film boiling [17] is extended to subcooled film boiling with wave motion, and the predictions by the extended model are compared with experimental results.

On the other hand, a numerical calculation is needed to know the heat transfer coefficients from the vapor-film-unit model. The development of a heat transfer correlation is thus effective to roughly estimate the heat transfer coefficients. For example, Sakurai [24] developed a heat transfer correlation of saturated film boiling along high vertical-surfaces based on the critical wave length of the Rayleigh–Taylor instability. However, it is not clear why the Rayleigh–Taylor instability plays a role in this film boiling system. In this report, based on the vapor-film-unit model, the reason is made clear, and a general heat transfer correlation is developed for film boiling with wave motion.

## 2. VAPOR-FILM-UNIT MODEL FOR SUBCOOLED FILM BOILING ALONG INCLINED AND VERTICAL SURFACES

In this section, the vapor-film-unit model for saturated film boiling developed by Nishio *et al.* [17] is extended to subcooled film boiling with wave motion along inclined and vertical surfaces, and the predictions by the extended model are compared with experimental data of the heat transfer coefficient obtained for film boiling along a high vertical surface.

### 2.1. Outline of vapor-film-unit model

Nishio *et al.* [17] observed the behavior of saturated film boiling of liquid nitrogen along a vertical flat-plate. They reported that a two-dimensional stationary vapor-dome existed at a small distance above the film boiling leading-edge and a two-dimensional wave departed periodically from the stationary vapor-dome. Based on such results of observation, they developed a vapor-film-unit model for saturated film boiling with wave motion along inclined and vertical surfaces. In the development of this previous model, the film boiling situation shown in Fig. 1 was imagined for vertical surfaces for example, and the following assumptions were employed.

(1) The vapor film is a series of two-dimensional vapor-film-units. The vapor-film-units are classified into the leading-edge and the upper vapor-film-units. The leading-edge vapor-film-unit is stationary and located near the film boiling leading-edge. A two-dimensional wave departs periodically from the leading-edge unit, and the waves form the upper vapor-film-units rising up along the surface at a constant velocity.

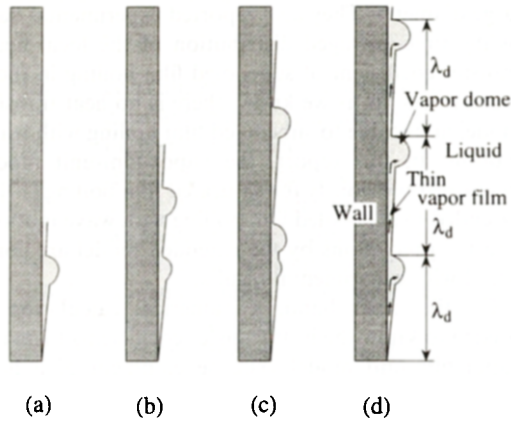


FIG. 1. Film boiling situation imagined in vapor-film-unit model for vertical surface.

(2) Each two-dimensional vapor-film-unit consists of a thin vapor film and a vapor dome. Since vapor generated in the thin vapor film is absorbed by the vapor dome located just above the thin vapor film, the film thickness just above the vapor dome becomes very thin. Every upper vapor-film-unit is therefore the same in heat transfer distribution and vapor-film-unit length as the leading-edge vapor-film-unit. The base size of the vapor dome is much smaller than the vapor-film-unit length.

(3) The vapor-film-unit length, which is the pitch between the vapor domes, is given by the most dangerous wavelength of the Kelvin-Helmholtz instability,  $\lambda_{d,KH}$ . This wavelength is determined by a stability analysis for the interface of the concurrent flow of vapor and liquid. As far as the wavelength is concerned, both fluids are treated incompressible and nonviscous, and the flow is irrotational. The effect of evaporation at the interface on the stability is negligible. The time-averaged thickness and velocity of the vapor flow,  $\delta_v$  and  $U_v$ , do not depend on the distance from the film boiling leading-edge  $x$ . The former is estimated as the thickness of the laminar-smooth vapor film at  $x = \lambda_{d,KH}$ , and the latter as the averaged vapor velocity at this point.

They reported that the vapor-film-unit length predicted from the model was in good agreement with experimental data of saturated liquid nitrogen and also that the model was applicable to predicting film-boiling heat transfer to saturated liquids along inclined and vertical surfaces. The assumptions listed above were thus also employed in the development of the present model. Following assumptions (1)–(3), the time-averaged local heat-transfer coefficient at  $x > \lambda_{d,KH}$  is given by

$$h = \frac{1}{\lambda_{d,KH}} \int_0^{\lambda_{d,KH}} h[x] dx \quad (1)$$

regardless of the distance from the film boiling leading-edge except for the leading-edge vapor-film-unit.

## 2.2. Determination of vapor-film-unit length

Following assumption (3), consider the vapor-liquid interface along an inclined flat-plate in the gravitational field and analyze the stability of the interface for the two-dimensional perturbation ( $y = \eta[t; x]$ ) as shown in Fig. 2.

If the fluctuation in the velocity potential is  $\Phi$ , the continuity equations of the vapor and the liquid flows are given by the following equations:

$$\nabla^2 \Phi_v = 0, \quad \nabla^2 \Phi_l = 0. \quad (2)$$

Applying the Bernoulli equation to the vapor and the liquid phases and eliminating second-order terms results in the following two equations:

$$-\frac{\partial \Phi_v}{\partial t} - U_v \frac{\partial \Phi_v}{\partial x} + \frac{p_v}{\rho_v} - g(\cos \phi)y = 0 \quad (3)$$

$$-\frac{\partial \Phi_l}{\partial t} - U_l \frac{\partial \Phi_l}{\partial x} + \frac{p_l}{\rho_l} - g(\cos \phi)y = 0 \quad (4)$$

where  $\phi$  is the inclination angle relative to the horizontal downward plane. The boundary conditions are as follows:

$$y = -\delta_v; \quad \frac{\partial \Phi_v}{\partial y} = 0 \quad (5)$$

$$y = \delta_l; \quad \frac{\partial \Phi_l}{\partial y} = 0 \quad (6)$$

$$y = 0; \quad -\frac{\partial \Phi_v}{\partial y} = \left(\frac{\partial \eta}{\partial t}\right) + U_v \left(\frac{\partial \eta}{\partial x}\right) \quad (7)$$

$$-\frac{\partial \Phi_l}{\partial y} = \left(\frac{\partial \eta}{\partial t}\right) + U_l \left(\frac{\partial \eta}{\partial x}\right) \quad (8)$$

$$p_v - p_l = -\sigma \left(\frac{\partial^2 \eta}{\partial x^2}\right). \quad (9)$$

Equations (2)–(9) are linear in the infinitesimal disturbance quantities, and therefore, considering only one Fourier component of the disturbance,  $\eta$ , as given by equation (10) will be sufficient in seeking a solution for  $\eta$ :

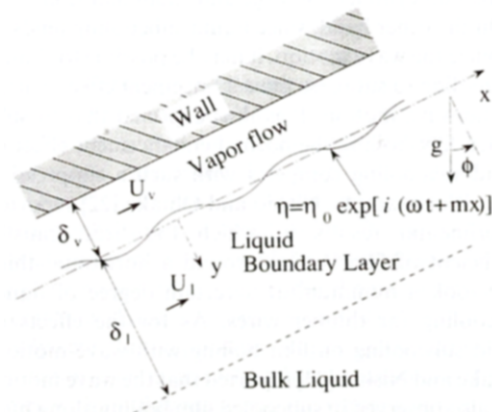


FIG. 2. Stability of vapor-liquid interface.

$$\eta = \eta_0 \exp [i(\omega t + mx)] \tag{10}$$

where 'i' is the unit complex number.

Now, substituting equation (10) in equation (2) and solving for  $\Phi_v$  and  $\Phi_l$  under the boundary conditions of equations (5)–(8), the following two equations are obtained:

$$\Phi_v = -i \left( \frac{\eta_0}{m} \right) (\omega + mU_v) \times \exp [i(\omega t + mx)] \frac{\cosh [m(y + \delta_v)]}{\sinh [m\delta_v]} \tag{11}$$

$$\Phi_l = i \left( \frac{\eta_0}{m} \right) (\omega + mU_l) \times \exp [i(\omega t + mx)] \frac{\cosh [m(y - \delta_l)]}{\sinh [m\delta_l]} \tag{12}$$

Next, by substituting equation (11) in equation (3) and equation (12) in equation (4), and using the boundary condition of equation (9), the following equation is obtained:

$$\rho_l(\omega + mU_l)^2 \coth [m\delta_l] + \rho_v(\omega + mU_v)^2 \coth [m\delta_v] - (\rho_l - \rho_v)g(\cos \phi)m = \sigma m^3 \tag{13}$$

Here, consider the following two cases:

Case 1;

$$m\delta_v \ll 1, \quad \delta_l \rightarrow \infty, \quad U_v = U_v, \quad U_l = 0 \tag{14}$$

Case 2;

$$m\delta_v \ll 1, \quad m\delta_l \ll 1, \quad U_v = U_v, \quad U_l = U_l \tag{15}$$

Under these two conditions, the wave-number at which the growth rate is maximum,  $m_d$ , is given by the following equations; for case 1,

$$m_d^4 + \frac{7\rho_{vf}}{3\rho_{lf}\delta_v} m_d^3 + \left( \frac{4\rho_{vf}^2}{3\rho_{lf}^2\delta_v^2} - \frac{\rho_{vf}U_v^2}{3\sigma\delta_v} + \frac{(\rho_{lf} - \rho_{vf})g \cos \phi}{3\sigma} \right) m_d^2 - \left( \frac{\rho_{vf}^2 U_v^2}{\sigma\rho_{lf}\delta_v^2} - \frac{\rho_{vf}(\rho_{lf} - \rho_{vf})g \cos \phi}{\rho_{lf}\sigma\delta_v} \right) m_d + \frac{2\rho_{vf}^2(\rho_{lf} - \rho_{vf})g \cos \phi}{3\rho_{lf}^2\sigma\delta_v^2} = 0 \tag{16}$$

and for case 2,

$$m = \frac{1}{\sqrt{2}} \sqrt{\left( \frac{\rho_{lf}\rho_{vf}(U_l - U_v)^2}{\sigma \left( \frac{\rho_{lf}}{\delta_l} + \frac{\rho_{vf}}{\delta_v} \right) \delta_l \delta_v} - \frac{(\rho_{lf} - \rho_{vf})g \cos \phi}{\sigma} \right)} \tag{17}$$

If the thickness and the velocities are given for the vapor and the liquid phases respectively, the most dangerous wavelength, which is the vapor-film-unit

length, is determined as  $\lambda_{d,KH} = 2\pi/m_d$  by using equation (16) or (17).

### 2.3. Determination of flow quantities

Following assumption (3) and the analytical results of the TPBL theory with an integral method by Nishio and Ohtake [22], the following equations are obtained for subcooled film boiling along an inclined flat-plate with the laminar-smooth vapor film:

$$\delta_v[x] = 2 \left( \frac{Sp^*}{Gr_v[x] Pr_{vf} \sin \phi} \right)^{1/4} \times \left[ \frac{1 - 2 \left( \frac{Sb}{Sp} \right) \left( \frac{Pr_{vf}}{Pr_{lf}} \right) \left( \frac{\delta}{\bar{\mu}} \right)}{1 + \frac{3 + Sp}{1 + 0.5Sp} a_v} \right]^{1/4} \tag{18}$$

$$\delta_l[x] = \frac{\delta_v}{\delta} \tag{19}$$

$$h[x] = \frac{1}{2} \left( \frac{k_{vf}}{x} \right) \left( \frac{Gr_v[x] Pr_{vf} \sin \phi}{Sp^*} \right)^{1/4} \times \left[ \frac{1 + \frac{3 + Sp}{1 + 0.5Sp} a_v}{1 - 2 \left( \frac{Sb}{Sp} \right) \left( \frac{Pr_{vf}}{Pr_{lf}} \right) \left( \frac{\delta}{\bar{\mu}} \right)} \right]^{1/4} \tag{20}$$

$$u_{v,av} = \frac{1}{\delta_v} \int_{-\delta_v}^0 u_v[x, y] dy = \frac{g(\sin \phi)(\rho_{lf} - \rho_{vf})\delta_v^2}{2\mu_{vf}} (1/6 + 0.5a_v) \tag{21}$$

where 'a<sub>v</sub>' is a constant relating to the vapor velocity. As for the mean velocity in the liquid boundary layer, it is given by the following equation if the liquid flow in the boundary layer is driven by shear force at the vapor-liquid interface and also buoyancy:

$$u_{l,av} = \frac{F\beta\Delta T_{sub}g\delta_l^2}{4\nu_{lf}} (\sin \phi) \left( \frac{a_l}{3} + \frac{1}{12} \right) \tag{22}$$

where 'a<sub>l</sub>' and 'F' are constants relating to the liquid velocity. In this case, the constants are determined by solving the following simultaneous equations:

$$a_v = \frac{1 + \left( \frac{F \cdot Sb}{2(1 - \bar{\rho})B} \right) \frac{1}{\delta}}{1 + 2 \left( \frac{\delta}{\bar{\mu}} \right)} \tag{23}$$

$$\delta^4 = \left( \frac{1+6a_1}{20} \right) \left( \frac{Sp^*}{Gr_v[x]Pr_{vf}} \right) \left( \frac{Pr_{lf}Sb}{B} \right) \left( \frac{gD^3}{v_{lf}^2} \right) \times \left[ \frac{1-2 \left( \frac{Pr_{vf}}{Pr_{lf}} \right) \left( \frac{Sb}{Sp} \right) \left( \frac{\delta}{\bar{\mu}} \right)}{1 + \frac{3+Sp}{1+0.5Sp} a_v} \right] F \quad (24)$$

$$a_1 = \frac{1+2 \frac{(1-\bar{\rho})B\delta^5}{F \cdot Sb}}{2 + \left( \frac{\bar{\mu}}{\delta} \right)} \quad (25)$$

$$\frac{1}{F} = \left( \frac{5}{7} \right) \left( \frac{1+7a_1+21a_1^2}{1+6a_1} \right) \left( \frac{1}{Pr_{lf}} \right) + \frac{3}{4}(1-2a_1). \quad (26)$$

If the liquid is driven only by the shear force, the mean liquid velocity is given by the following equation:

$$u_{l,av} = \frac{g \sin \phi (\rho_{lf} - \rho_{vf}) \delta_v^2}{6\mu_{vf}} a_v. \quad (27)$$

In this case, the constants are determined by solving the following simultaneous equations:

$$a_v = \frac{\bar{\mu}}{(\bar{\mu} + 2\delta)} \quad (28)$$

$$\delta^3 + \frac{1}{2} \left\{ 1 + \left( \frac{3+Sp}{1+0.5Sp} \right) \right\} \bar{\mu} \delta^2 + \left( \frac{3Sp^*Sb\bar{\mu}}{5\bar{\rho}Sp} \right) \delta - \left( \frac{3Pr_{lf}Sp^*\bar{\mu}^2}{10Pr_{vf}\bar{\rho}} \right) = 0. \quad (29)$$

In this study, the mean liquid velocity was determined by equation (22).

In our previous report [17], it was shown that the predictions by the vapor-film-unit model were in good agreement with experimental data of saturated film boiling if the flow quantities in equation (16) were given as:

$$U_v = u_{v,av}[x = \lambda_{d,KH}], \quad \delta_v = \delta_v[x = \lambda_{d,KH}]. \quad (30)$$

In this report, thus, the flow quantities in equations (16) and (17) are estimated by equations (30) and (31)

$$U_l = u_{l,av}[x = \lambda_{d,KH}], \quad \delta_l = \delta_l[x = \lambda_{d,KH}]. \quad (31)$$

For example, the following values of  $\delta_v$  and  $\delta_l$  at  $x = \lambda_{d,KH}$  are obtained for film boiling of freon R113 along a vertical plate from equations (18) and (19) under the conditions of equations (30) and (31)

$$\Delta T_{sub} = 10 \text{ K}; \quad m_d \delta_v = 0.0742, \quad m_d \delta_l = 0.123$$

$$\Delta T_{sub} = 20 \text{ K}; \quad m_d \delta_v = 0.0445, \quad m_d \delta_l = 0.107$$

$$\Delta T_{sub} = 30 \text{ K}; \quad m_d \delta_v = 0.0283, \quad m_d \delta_l = 0.0984.$$

Thus, equation (15) (Case 2) is expected to be applicable to subcooled film boiling, and equation (14) (Case 1) for saturated film boiling. It should be noted

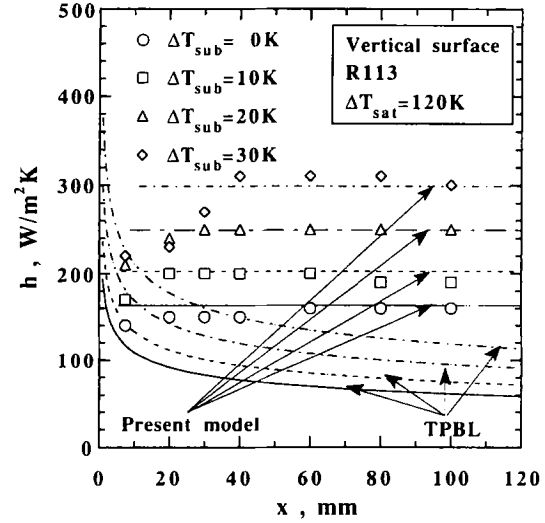


FIG. 3. Comparison of experimental results [23] with predictions by the present model and the TPBL theory for distribution of time-averaged local heat-transfer coefficient of film boiling along vertical surface.

that the most dangerous wavelengths calculated for Cases 1 and 2 are not so different from each other for this example.

#### 2.4. Comparison with experimental data

In Fig. 3, the time-averaged local heat-transfer coefficients of film boiling along a vertical surface predicted by the present model are compared with experimental data of freon R113 at  $\Delta T_{sat} = 120 \text{ K}$  obtained by Ohtake and Nishio [23]. In this figure, the predictions by the TPBL theory are also plotted. In Fig. 4, the experimental data of the local heat-transfer coefficient at  $x = 60 \text{ mm}$  are plotted against the wall superheat together with the predictions by the present model. As seen from these figures, the

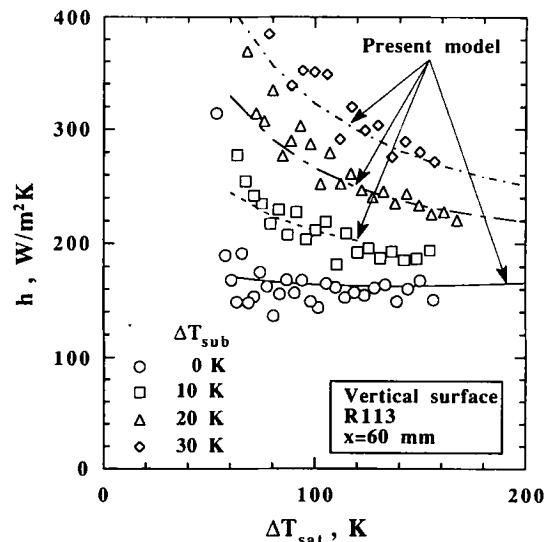


FIG. 4. Comparison of experimental results [23] with predictions by the present model for wall-superheat dependence of time-averaged local heat-transfer coefficient of film boiling along vertical surface.

present vapor-film-unit model can describe correctly the effects of the distance, liquid subcooling, and wall superheat on the time-averaged local heat-transfer coefficient except for a region near the film boiling leading-edge.

### 3. EXTENSION OF THE VAPOR-FILM-UNIT MODEL TO SUBCOOLED FILM BOILING AROUND HORIZONTAL CYLINDERS OF LARGE DIAMETER

In this section, the vapor-film-unit model described in the previous section is extended to subcooled film boiling around horizontal cylinders of large diameter.

#### 3.1. Outline of the model

First, the vapor-film-unit length for film boiling along an inclined flat-plate at a prescribed subcooling,  $\lambda = \lambda_{d,KH}$ , was calculated from equation (16) or (17) as a function of the inclination angle relative to the horizontal downward plane,  $\phi$ . As shown by Nishio *et al.* [17] for saturated film boiling, the results of this calculation show that the vapor-liquid interface is stable for the angular region from  $\phi = 0$  to a certain angle  $\phi_{st}$ . In the present model, thus, the first two-dimensional vapor dome is placed at  $\phi = \phi_{st} = \phi_1$ , where the value of  $\phi_{st}$  depends on liquid subcooling. The vapor film between  $0 < \phi < \phi_1$ , forms the first vapor-film-unit corresponding to the leading-edge vapor-film-unit in the case of film boiling along vertical surfaces. Next, for  $\phi > \phi_{st}$ , the value of  $\phi_2$  is determined by the following equation with  $n = 2$ , and the second vapor dome is placed at  $\phi = \phi_2$ :

$$\frac{D}{2} (\phi_n - \phi_{n-1}) = \frac{1}{(\phi_n - \phi_{n-1})} \int_{\phi_{n-1}}^{\phi_n} \lambda_{d,KH}[\phi] d\phi. \quad (32)$$

The vapor film between  $\phi_1 < \phi < \phi_2$  forms the second vapor-film-unit. Repeating this procedure, as many complete vapor-film-units as possible are placed around the cylinder periphery and then the total arrangement of the vapor film units is determined.

As mentioned later, observation of the vapor-liquid interface around the cylinder showed that the vapor domes moved up along the periphery with time and the arrangement of the vapor film units showed a cyclic behavior. In the present model, to take into account this cyclic behavior of the arrangement, the vapor domes are moved as shown in Fig. 5. First, the

initial arrangement in the cycle ( $t = 0$ ) is given as the arrangement stated above. Next, the first vapor dome is moved from  $\phi_1$  to  $\phi'_1 = \phi_1 + \alpha = \phi_{st} + \alpha$  as shown in Fig. 5, where  $\alpha$  is an infinitesimal angle. The location of the second dome at this time,  $\phi'_2$ , is determined as  $\phi'_2 = \phi_2$  by equation (32) with  $n = 2$  and  $\phi_1 = \phi'_1$ . The locations of other upper domes at this time are determined in the same way. Repeating this procedure by increasing  $\alpha$ , the instantaneous arrangement of the vapor-film-units in the cycle is determined until the first dome reaches the initial location of the second dome ( $\phi'''_1 = \phi_2$  in Fig. 5). When the first dome reaches the initial location of the second dome ( $t = t_3$ ), the arrangement is back to the initial arrangement ( $t = 0$ ).

The distribution of the heat transfer coefficient in the first vapor-film-unit is estimated by the TPBL theory with an integral method for subcooled film boiling around the cylinder [22]. As for other upper vapor-film-units, the instantaneous local heat-transfer coefficient at  $\phi$  is estimated approximately by equation (20) with the value of  $x$  measured from the front of the vapor-film-unit covering the point. The distribution of the time-averaged local heat-transfer coefficient is then obtained by averaging the instantaneous local heat-transfer coefficient over the cycle.

#### 3.2. Comparison with experimental data

In Fig. 6, the predictions of the time-averaged local heat-transfer coefficient of film boiling around a horizontal cylinder of  $D = 50.8$  mm are compared with the experimental data of freon R113 at  $\Delta T_{sat} = 120$  K obtained by Ohtake and Nishio [23],  $h_{ex}$ . In Fig. 7, they are compared for  $D = 16$  mm. In these figures, the predictions by the TPBL theory are also plotted. As seen from the figures, the present vapor-film-unit model can describe correctly the distribution of the time-averaged local heat-transfer coefficient of film boiling around horizontal cylinders of large diameter. In particular, it can describe the following experimental results for film boiling around horizontal cylinders of large diameter obtained by Ohtake and Nishio [23]; the distribution of the time-averaged local heat-transfer coefficient is almost uniform for saturated film boiling regardless of the cylinder diameter, but it becomes to take a maximum at about  $\phi = 90$  deg with increasing both the liquid subcooling and the cylinder diameter.

In Fig. 8, for freon R113, the predictions of the heat transfer coefficient averaged over the periphery of the cylinder are plotted against the cylinder diameter together with the experimental data at  $\Delta T_{sat} = 120$  K and the predictions by the TPBL theory. Fig. 9 shows the comparison with the experimental data of saturated film boiling for freon R113 and iso-propanol obtained by Breen and Westwater [2]. As seen from these figures, the present model can predict the averaged heat-transfer coefficient and also the experimental result that the averaged value is independent of the cylinder diameter in the large diameter region.

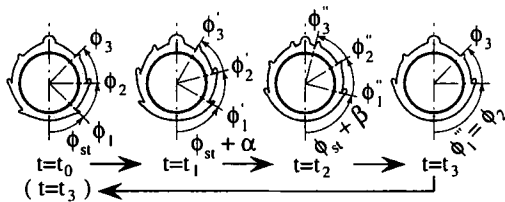


FIG. 5. Film boiling situation imagined in vapor-film-unit model for film boiling around horizontal cylinder of large diameter.

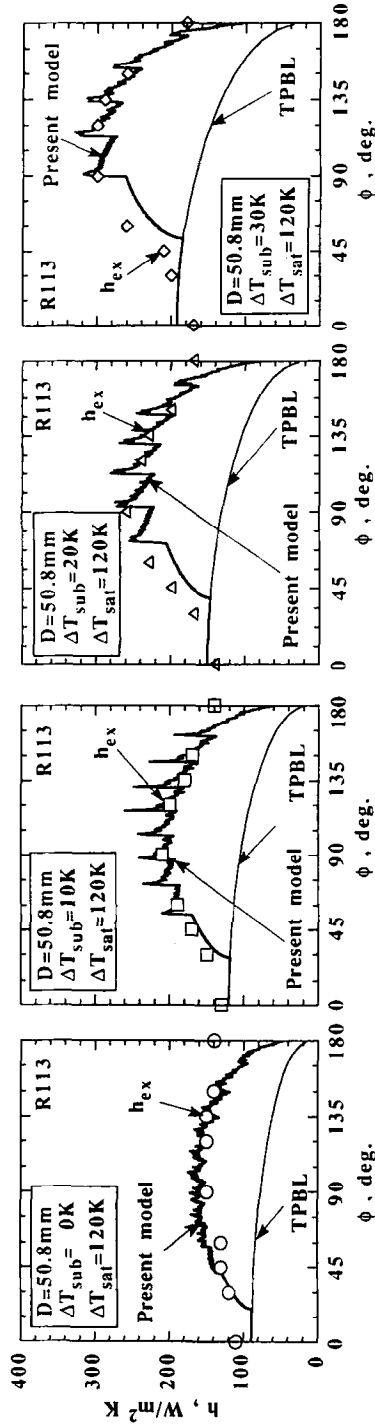


Fig. 6. Comparison of experimental results [23] with predictions by the present model and the TPBL theory for distribution of time-averaged local heat-transfer coefficient of film boiling around horizontal cylinder of  $D = 50.8$  mm.

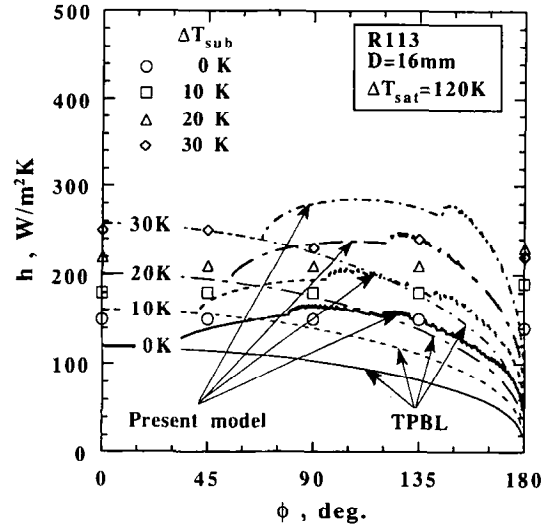


FIG. 7. Comparison of experimental results [23] with predictions from the present model and the TPBL theory for distribution of time-averaged local heat-transfer coefficient of film boiling around horizontal cylinder of  $D = 16$  mm.

3.3. Observation of behavior of vapor-liquid interface

Summarizing the results obtained above, the present vapor-film-unit model can describe correctly the effects of liquid subcooling, wall superheat, the geometry and the size of the heat transfer surface on natural-convection film-boiling with wave motion. However, many assumptions were employed in the development of the model. Thus, in this section, the behavior of the vapor-liquid interface is observed to check the model.

The test surface used in this observation is shown schematically in Fig. 10. To make the observation of behavior of the interface easy, a short horizontal

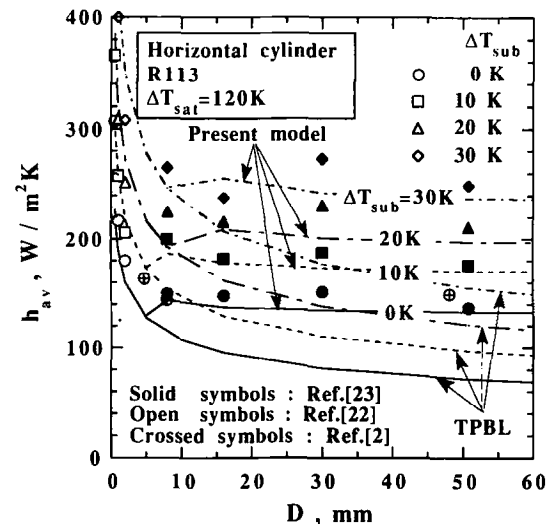


FIG. 8. Comparison of experimental results with predictions from the present model and the TPBL theory for diameter dependence of averaged heat-transfer coefficient of film boiling around horizontal cylinder.



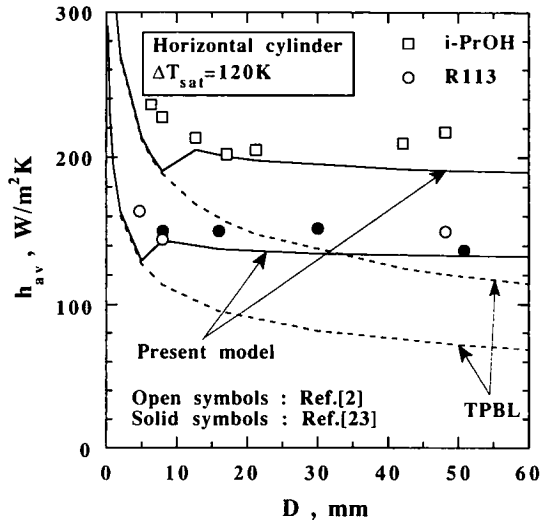


FIG. 9. Comparison of experimental results with predictions from the present model and the TPBL theory for diameter dependence of averaged heat-transfer coefficient of saturated film boiling around horizontal cylinder.

cylinder of stainless steel was used as the test surface. The cylinder was 50.8 mm in diameter, 15 mm in length, and 1.5 mm in thickness. Teflon (PTFE) sheets of 0.5 mm thickness were bonded to the sides of the cylinder. A K-type thermocouple was spot-welded at  $\phi = 90$  deg from inside the cylinder. The test cylinder was heated up to about 250°C in an electric hearth. After that, the cylinder was immersed into a bath of freon R113 kept at a prescribed subcooling and it was cooled down in the bath. The behavior of the vapor-liquid interface during the quenching test was recorded by a video recorder.

Results of the observation showed that the wave motion similar to the situation shown in Fig. 5 appeared. Figure 11 shows experimental results of the values of  $\phi_{st} = \phi_1$  and  $\phi_\lambda = \phi_n - \phi_{n-1}$ , where  $\phi_\lambda$  is the angular region of the vapor-film-unit located at about  $\phi = 90$  deg. In the figure, the predictions from the present model are also plotted together with the

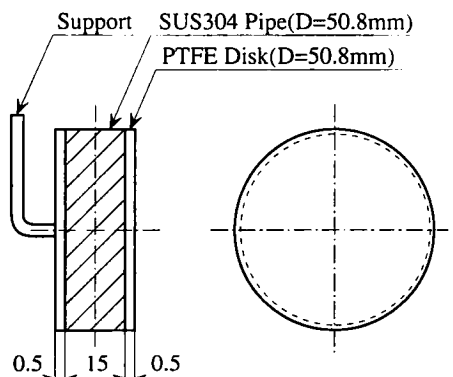


FIG. 10. Schematic diagram of test surface for observation of vapor-liquid interface.

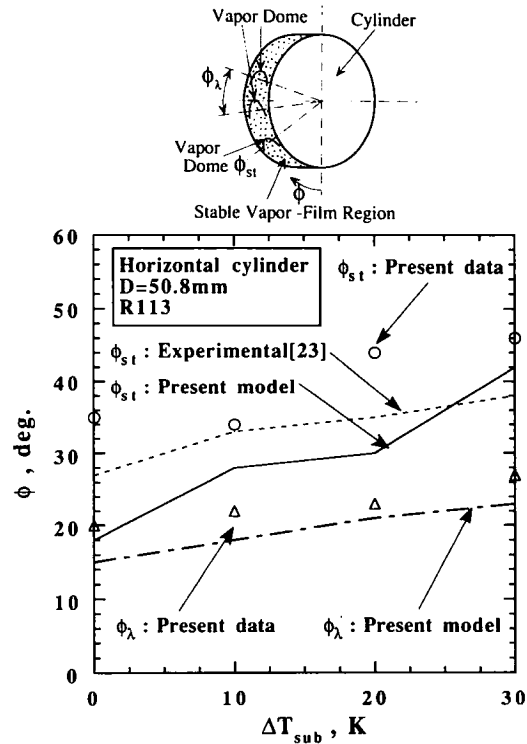


FIG. 11. Comparison of predicted values of angular location of vapor domes with experimental data.

experimental data obtained by Ohtake and Nishio [23]. As seen from the figure, the predicted results are in agreement with the experimental data.

#### 4. HEAT TRANSFER CORRELATION OF FILM BOILING WITH WAVE MOTION

As mentioned already, Sakurai [24] presented a heat transfer correlation for saturated film boiling along high vertical surfaces. In this correlation, the critical wavelength of the Rayleigh-Taylor instability,  $\lambda_{c,RT}$ , is included as the representative length. However, the physical meaning of this length is not clear because the Rayleigh-Taylor instability is not expected to appear in film boiling along vertical surfaces. Based on the vapor-film-unit model, first, the physical meaning is investigated.

Substituting equations (18) and (21) in equation (16) and assuming  $\rho_v/\rho_l \ll 1$  and  $a_v = 0$ , the most dangerous wavelength,  $\lambda_{d,KH}$ , for saturated film boiling along a vertical surface is given by

$$\lambda_{d,KH} = \lambda = 16.2 \left( \frac{Pr_{vf}^3}{Sp^{*3} Gr_v[\lambda_0]} \right)^{1/11} \lambda_0 \quad (33)$$

where  $\lambda_0$  is the Laplace capillary length. This equation indicates that the vapor-film-unit length of saturated film boiling along a vertical surface closely relates to the Laplace capillary length. Since the critical wavelength of the Rayleigh-Taylor instability is proportional to the Laplace capillary length, the vapor-

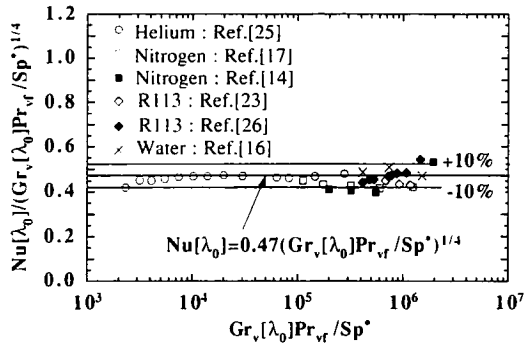


FIG. 12. Heat transfer correlation for saturated film boiling along vertical surface based on Laplace capillary length.

film-unit model predicts that the heat transfer coefficient of saturated film boiling along a high vertical surface relates to the critical wavelength,  $\lambda_{c,RT}$ . For example, experimental data of  $Nu[\lambda_0]/(Gr_v[\lambda_0]Pr_{vf}/Sp^*)^{1/4}$  for vertical surfaces [14, 16, 17, 23, 25, 26] are plotted to  $Gr_v[\lambda_0]Pr_{vf}/Sp^*$  in Fig. 12 because most of the TPBL theories result in the form

$$Nu[s] = \text{const.} \left( \frac{Gr_v[s]Pr_{vf}}{Sp^*} \right)^{1/4} \quad (34)$$

where 's' is the representative length. As seen from this figure, saturated film-boiling heat transfer along high vertical-surfaces can be correlated to the Laplace capillary length.

Based on this result, the experimental data in Fig. 12 are replotted in Fig. 13 by taking the representative length as the vapor-film-unit length given by equation (33). From this figure, the following equation is obtained as the heat transfer correlation of saturated film boiling along high vertical-surfaces:

$$Nu[\lambda] = 0.74 \left( \frac{Gr_v[\lambda]Pr_{vf}}{Sp^*} \right)^{1/4} \quad (35)$$

For the liquids shown in Figs. 12 and 13, the vapor-film-unit length given by equation (33) is almost equal to the critical wavelength of the Rayleigh–Taylor instability,  $\lambda_{c,RT}$ . For this case, thus, the vapor-film-unit length in equation (35),  $\lambda$ , can be replaced by

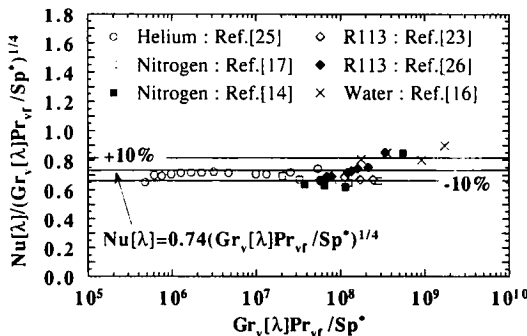


FIG. 13. Heat transfer correlation for saturated film boiling along vertical surface based on vapor-film-unit length.

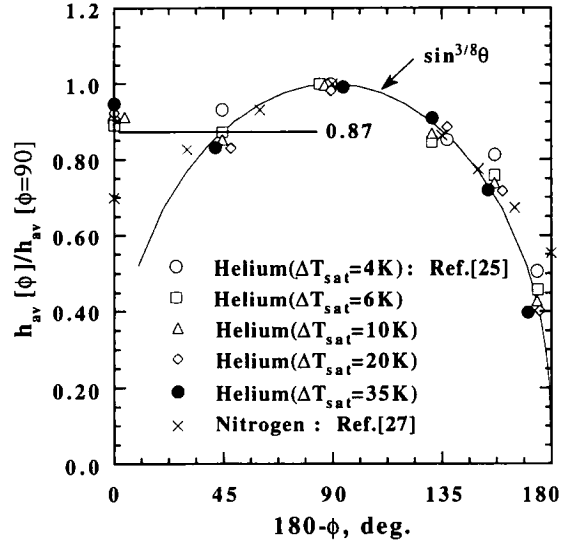


FIG. 14. Comparison of experimental results for saturated film boiling along inclined flat-plate with general heat-transfer correlation.

$\lambda_{c,RT} = 2\pi\lambda_0$ . In this case, equation (35) becomes

$$Nu[\lambda_0] = 0.47 \left( \frac{Gr_v[\lambda_0]Pr_{vf}}{Sp^*} \right)^{1/4} \quad (36)$$

Since equation (35) was obtained on the basis of the vapor-film-unit length, there is a possibility that equation (35) is applicable also to other saturated film-boiling systems with wave motion. For saturated film boiling on horizontal flat-plates facing upward, Berenson [19] showed that the vapor-film-unit length was given by the most dangerous wavelength of the Rayleigh–Taylor instability,  $\lambda_{d,RT}$ . If  $\lambda = \lambda_{d,RT}$  is substituted in equation (35), the following equation is obtained:

$$Nu[\lambda_0] = 0.41 \left( \frac{Gr_v[\lambda_0]Pr_{vf}}{Sp^*} \right)^{1/4} \quad (37)$$

The equation obtained by replacing the proportionality constant in this equation (0.41) by 0.425 is the same one that Berenson [19] derived semi-analytically. This result means that equation (35) is also applicable to saturated film boiling on horizontal flat-plates facing upward. Taking the ratio of equation (37) to equation (36), the following relation is obtained:

$$\frac{h_{av}[\phi = 90 \text{ deg}]}{h_{av}[\phi = 180 \text{ deg}]} = 0.87. \quad (38)$$

As for saturated film boiling along inclined flat-plates, the gravitational acceleration in  $\lambda_0$  and  $Gr_v[\lambda_0]$ ,  $g$ , should be replaced by  $g(\sin \phi)$  because it means the buoyancy driving the vapor flow. By this replacement in equation (35), the following relation is obtained for saturated film boiling along inclined flat-plates:

$$\frac{h_{av}[\phi]}{h_{av}[\phi = 90 \text{ deg}]} = (\sin \phi)^{3/8}. \quad (39)$$

The relations of equations (38) and (39) are compared with experimental data obtained by Nishio and Chandratilleke [25] and Sauer and Lin [27] in Fig. 14. As

seen from this figure, equations (38) and (39) are in good agreement with the experimental results. Equation (35) is thus also applicable to saturated film boiling along inclined flat plates.

In Fig. 15, equation (35) with  $\lambda = \lambda_{c,RT}$  is compared with experimental data of saturated film boiling around horizontal cylinders of large diameter [23]. It is seen from the figure that equation (35) is also applicable to saturated film boiling around horizontal cylinders if the vapor-film-unit length is taken as  $\lambda = \lambda_{c,RT}$ .

Summarizing the results stated above, it can be concluded that equation (35), which is derived from the vapor-film-unit model, is expected generally applicable to saturated film boiling with wavy motion if the vapor-film-unit length is given adequately.

Finally, a heat transfer correlation of subcooled film boiling with wave motion is derived. Nishio *et al.* [28] developed the following heat transfer correlation for subcooled film boiling with the laminar-smooth vapor film

$$h_{sub} = h_{sat} + 0.067 \left( \frac{k_{vf}}{s} \right) \left( \frac{Pr_{lf}^{0.21}}{\rho\mu^{0.23}} \right) (Gr_l[s] Pr_{lf})^{1/4} \frac{\Delta T_{sub}}{\Delta T_{sat}} \quad (40)$$

The calculated results of this equation are plotted in Figs. 15 and 16 together with experimental data [23]. In these figures, the value of  $h_{sat}$  was estimated from equation (35), and the length scale in  $Gr_l[s]$  was taken as the vapor-film-unit length given by equation (33). While, the predictions in Fig. 16 show the subcooling-dependence a little weaker than that of the data, it is considered that equation (40) works well also for subcooled film boiling with wave motion.

### 5. CONCLUSIONS

In this report, the vapor-film-unit model focusing on the vapor-film-unit length was developed for sub-

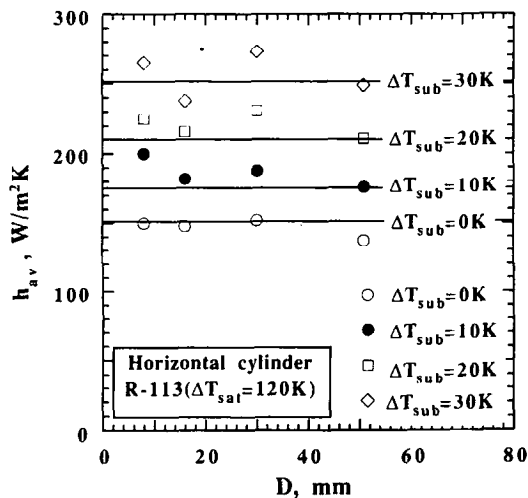


FIG. 15. Comparison of experimental results [23] for saturated and subcooled film boiling around horizontal cylinder of large diameter with general heat-transfer correlation.

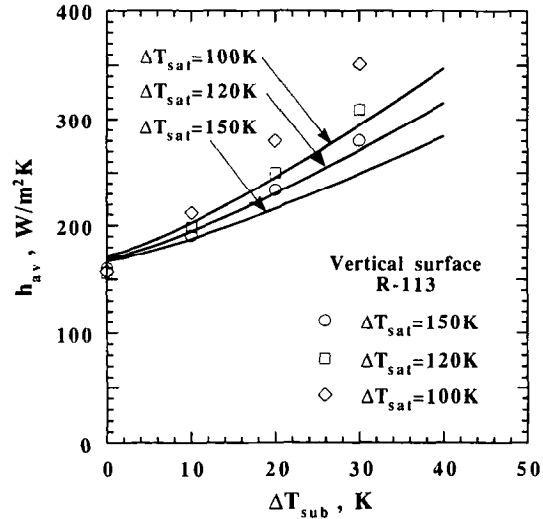


FIG. 16. Comparison of experimental results [23] for saturated and subcooled film boiling along vertical surface with general heat-transfer correlation.

cooled film boiling with interfacial wave motion along inclined and vertical surfaces. Next, the model was extended to subcooled film boiling with wave motion around horizontal cylinders. Comparison of the predictions by the model with experimental results showed that the present model works well for film-boiling heat transfer with wave motion. In addition, observation of the wave motion was conducted, and it was found that the actual situation of the wave motion is similar to that assumed in the model. Based on the present vapor-film-unit model, it was shown that the vapor-film-unit length along a vertical plate relates basically to the Laplace capillary length and it is approximately equal to the critical wavelength of the Rayleigh–Taylor instability. Finally, a general form of heat transfer correlation based on the vapor-film-unit length of the present model was derived.

### REFERENCES

1. E. K. Kalinin, I. I. Berlin and V. V. Kostyuk, Film-boiling heat transfer, *Advances in Heat Transfer*, Vol. 11, pp. 51–197. Academic Press, New York (1975).
2. B. P. Breen and J. W. Westwater, Effect of diameter of horizontal tubes on film boiling heat transfer, *Chem. Eng. Prog.* **58**, 67–72 (1962).
3. L. A. Bromley, Heat transfer in stable film boiling, *Chem. Eng. Prog.* **46**, 221–227 (1950).
4. K. Nishikawa and T. Ito, Two-phase boundary-layer treatment of free-convection film boiling, *Int. J. Heat Mass Transfer* **9**, 103–115 (1966).
5. K. Nishikawa, T. Ito, T. Kuroki and K. Matsumoto, Pool film boiling heat transfer from a horizontal cylinder to saturated liquids, *Int. J. Heat Mass Transfer* **15**, 853–962 (1972).
6. K. Nishikawa, T. Ito and K. Matsumoto, Investigation of variable thermophysical property problem concerning pool film boiling from vertical plate with prescribed uniform temperature, *Int. J. Heat Mass Transfer* **19**, 1173–1181 (1976).
7. A. Sakurai, M. Shiotsu and K. Hata, Effect of subcooling

- on film boiling heat transfer from horizontal cylinder in a pool of water, *Heat Transfer 1986* **4**, 2043–2048 (1986).
8. T. H. K. Frederking and J. A. Clark, Natural convection film boiling on a sphere, *Adv. Cryogenic Eng.* **8**, 501–505 (1963).
  9. V. K. Dhir and G. P. Purohit, Subcooled film-boiling heat transfer from spheres, *Nucl. Eng. Des.* **47**, 49–66 (1978).
  10. M. M. Farahat and T. N. Nasr, Natural convection film boiling from spheres to saturated liquids: An integral approach, *Int. J. Heat Mass Transfer* **21**, 256–258 (1978).
  11. S. Nishio, Y. Himeji and V. K. Dhir, Natural-convection film-boiling heat transfer (2nd report: Film boiling from a horizontal flat plate facing downward), *Proc. 1991 ASME/JSME Thermal Eng. Joint Conf.*, Vol. 2, pp. 275–280. Hemisphere, New York (1991).
  12. E. R. Hosler and J. W. Westwater, Film boiling on a horizontal plate, *ARS J.* **32**, 553–558 (1962).
  13. Y. Y. Hsu and J. W. Westwater, Approximate theory for film boiling on vertical surface, *Chem. Eng. Prog. Symp. Ser.* **56**(30), 15–24 (1960).
  14. N. V. Suryanarayana and H. Merte, Jr., Film boiling on vertical surfaces, *ASME J. Heat Transfer* **94**, 377–384 (1972).
  15. E. M. Greitzer and F. H. Abernathy, Film boiling on vertical surfaces, *Int. J. Heat Mass Transfer* **15**, 475–491 (1972).
  16. T. D. Bui and V. K. Dhir, Film boiling heat transfer on an isothermal vertical surface, *ASME J. Heat Transfer* **107**, 764–771 (1985).
  17. S. Nishio, G. R. Chandratilleke and T. Ozu, Natural-convection film-boiling heat transfer (1st report: Saturated film boiling with long vapor film), *JSME Int. J. (Series II)* **34**, 202–211 (1991).
  18. G. E. Coury and A. E. Dukler, Turbulent film boiling on vertical surfaces; A study including the influence of interfacial waves. In *Heat Transfer 1970* (Edited by U. Grigull and E. Hahne), Vol. 5, B3.6. Elsevier, Amsterdam (1970).
  19. P. J. Berenson, Film-boiling heat transfer from a horizontal surface, *ASME J. Heat Transfer* **83**, 351–358 (1961).
  20. J. G. M. Andersen, Low-flow film boiling heat transfer on vertical surfaces (Part I: Theoretical model), *A.I.Ch.E. Symp. Ser.* **73**(164), 2–6 (1976).
  21. K. J. Baumeister and T. D. Hamill, Laminar flow analysis of film boiling from a horizontal wire, NASA TN D-4035 (1967).
  22. S. Nishio and H. Ohtake, Natural-convection film-boiling heat transfer (3rd report: Film boiling from horizontal cylinder in middle- and small-diameter regions), *JSME Int. J. (Series II)* **35**, 580–588 (1992).
  23. H. Ohtake and S. Nishio, Natural-convection film-boiling heat transfer (4th report: Experiments of subcooled film boiling with long vapor film), *JSME Int. J. (Series II)* (in press).
  24. A. Sakurai, Film boiling heat transfer. In *Heat Transfer 1990* (Edited by G. Hetsroni), Vol. 1, pp. 157–187. Hemisphere, New York (1990).
  25. S. Nishio and G. R. Chandratilleke, Steady-state pool boiling heat transfer to saturated liquid helium at atmospheric pressure, *JSME Int. J. (Series II)* **32**, 639–645 (1989).
  26. S.-P. Liaw and V. K. Dhir, Effect of surface wettability on transition boiling heat transfer from a vertical surface. In *Heat Transfer 1986* (Edited by C. L. Chen, V. P. Carey and J. K. Ferrell), Vol. 4, pp. 2031–2036. Hemisphere, New York (1986).
  27. H. J. Sauer, Jr., and S.-C. Lin, Effect of inclination on film boiling heat transfer. In *Heat Transfer 1974* (Edited by T. Mizushima), Vol. 4, pp. 110–114. JSME-SCEJ, Tokyo (1974).
  28. S. Nishio, M. Uemura and K. Sakaguchi, Film boiling heat transfer and minimum-heat-flux-point condition in subcooled pool boiling, *JSME Int. J. (Series II)* **30**, 1274–1281 (1987).